

AD-A189 256

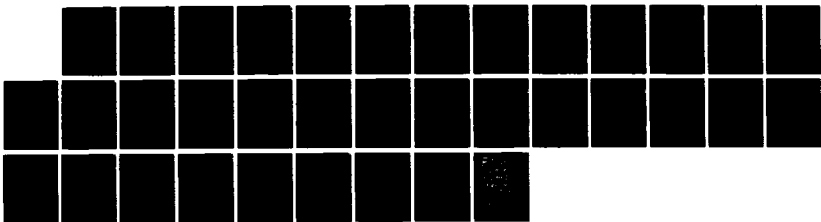
THE TOPOLOGICAL ASPECTS OF IMMUNOLOGICAL CONTROL  
NETWORKS(U) GEORGIA UNIV ATHENS DEPT OF CHEMISTRY  
R B KING 11 DEC 87 TR-55 N00014-84-K-0365

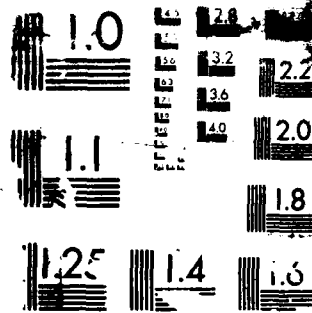
1/1

UNCLASSIFIED

F/G 6/5

NL





RESOLUTION TEST CHART

DTIC FILE COPY

4

OFFICE OF NAVAL RESEARCH

Contract NO0014-84-K-0365

R&T Code 4007001-6

Technical Report No. 55

Topological Aspects of Immunological Control Networks

by

R. Bruce King

Prepared for Publication

in the

International Journal of Mathematical Modelling

AD-A189 256

University of Georgia  
Department of Chemistry  
Athens, Georgia 30602

December 11, 1987

Reproduction in whole or in part is permitted for  
any purpose of the United States Government

This document has been approved for public release  
and sale; its distribution is unlimited.

DTIC  
ELECTE  
DEC 29 1987  
S H

27

8

Unclassified

SECURITY CLASSIFICATION OF THIS PAGE (When Data Entered)

REPORT DOCUMENTATION PAGE		READ INSTRUCTIONS BEFORE COMPLETING FORM
1. REPORT NUMBER Technical Report No. 55	2. GOVT ACCESSION NO. AD-A189256	3. RECIPIENT'S CATALOG NUMBER
4. TITLE (and Subtitle) Topological Aspects of Immunological Control Networks	5. TYPE OF REPORT & PERIOD COVERED	
	6. PERFORMING ORG. REPORT NUMBER	
7. AUTHOR(s) R.B. King	8. CONTRACT OR GRANT NUMBER(s) N00014-84-K-0365	
9. PERFORMING ORGANIZATION NAME AND ADDRESS University of Georgia Department of Chemistry Athens, GA 30602	10. PROGRAM ELEMENT, PROJECT, TASK AREA & WORK UNIT NUMBERS 4007001-6	
11. CONTROLLING OFFICE NAME AND ADDRESS Office of Naval Research Department of the Navy Arlington, VA 22217	12. REPORT DATE December 11, 1987	
	13. NUMBER OF PAGES 29	
14. MONITORING AGENCY NAME & ADDRESS (if different from Controlling Office)	15. SECURITY CLASS. (of this report)	
	15a. DECLASSIFICATION/DOWNGRADING SCHEDULE	
16. DISTRIBUTION STATEMENT (of this Report) This document has been approved for public release and sale; its distribution is unlimited.		
17. DISTRIBUTION STATEMENT (of the abstract entered in Block 20, if different from Report)		
18. SUPPLEMENTARY NOTES To be published in the "International Journal of Mathematical Modelling."		
19. KEY WORDS (Continue on reverse side if necessary and identify by block number) Immunology, Topology, Bipartite Graphs, Kinetic Logic, Herzenberg Models		
20. ABSTRACT (Continue on reverse side if necessary and identify by block number) Immunological control networks can be modelled by bipartite signed directed graphs called influence diagrams. Possible flow topologies around unstable steady states in such systems can be determined by kinetic logic based on the directed Boolean cubes of switching circuit theory. This method can identify the stable "help" and "suppression" configurations of the basic Herzenberg core regulatory circuit as well as the "memory" and "non-responsive" configurations of the model of Kaufman, Urbain, and Thomas. Furthermore, addition of a single vertex to the Herzenberg core regulatory circuit so as to preserve the bipartite nature of the signed directed graph leads to a network with		

DD FORM 1473  
1 JAN 73

EDITION OF 1 NOV 68 IS OBSOLETE  
S N 0102-LF-014-6601

Unclassified

SECURITY CLASSIFICATION OF THIS PAGE (When Data Entered)

Unclassified

SECURITY CLASSIFICATION OF THIS PAGE (When Data Entered)

five independent internal variables and two connected feedback circuits, either positive and negative circuits of length 4 or positive circuits of lengths 4 and 2. The flow topology of either of these systems indicates that addition of the fifth vertex switches the basic four-vertex core regulatory circuit into one of its two stable configurations.



Approval for

by

DATE

A-1

S/N 0102-LF-014-6601

Unclassified

SECURITY CLASSIFICATION OF THIS PAGE (When Data Entered)

TOPOLOGICAL ASPECTS OF IMMUNOLOGICAL CONTROL NETWORKS

R.B. King

Department of Chemistry

University of Georgia

Athens, Georgia 30602

U.S.A.

## Abstract

Immunological control networks can be modelled by bipartite signed directed graphs called *influence diagrams*. Possible flow topologies around unstable steady states in such systems can be determined by kinetic logic based on the directed Boolean cubes of switching circuit theory. This method can identify the stable "help" and "suppression" configurations of the basic Herzenberg core regulatory circuit as well as the "memory" and "non-responsive" configurations of the model of Kaufman, Urbain, and Thomas. Furthermore, addition of a single vertex to the Herzenberg core regulatory circuit so as to preserve the bipartite nature of the signed directed graph leads to a network with five independent internal variables and two connected feedback circuits, either positive and negative circuits of length 4 or positive circuits of lengths 4 and 2. The flow topology of either of these systems indicates that addition of the fifth vertex switches the basic four-vertex core regulatory circuit into one of its two stable configurations.

## 1. Introduction

A research area of major interest to immunologists is the nature and extent of the interactions that regulate the quantity of antibody secreting cells produced in response to antigen. In this connection network theory has been used by a number of workers to model such interactions. The general objective of this paper is the examination of such immunological control networks using topological and graph-theoretical methods similar to those previously used for chemical reaction networks (King, 1980, 1982, 1983). Such methods are based on kinetic logic (Thomas, 1979) and in the case of immunological control networks use the flow topology in Boolean or logical variable space to identify which of the proposed networks can exhibit stable configurations corresponding to the experimentally observed "memory" and "non-responsive" states (Kaufman, Urbain, and Thomas, 1985). The extension of these methods from chemical to immunological control networks is not trivial since the general patterns of immunological control networks are quite different from those of chemical reaction networks. Immunological control networks treated in this paper include those which can be modelled using no more than five variables. Such networks include networks proposed by Herzenberg, Black, and Herzenberg (1980); Kaufman, Urbain, and Thomas (1985); Hiernaux (1977); and Richter (1978a, b). Other networks such as the "plus-minus" network of Hoffmann (1978) require a larger number of variables and interactions and therefore are not as conveniently treated by the methods outlined in this paper.

Two research groups have recently published work on immunological control networks using methods related to those discussed in this paper. Kaufman, Urbain, and Thomas (1985) have used a similar but not identical flow topological analysis also based on the ideas of kinetic logic to evaluate one of the models also discussed

in this paper. Eisenfeld and DeLisi (Eisenfeld and DeLisi, 1985; Eisenfeld, 1986) have analyzed the qualitative stability of immunological control networks using network diagrams to depict essential topological relationships and mathematical methods related to those used by Clarke (1980) for the study of chemical reaction networks. This paper extends the approach of Eisenfeld and DeLisi by considering the flow topologies rather than the stabilities of immunological control networks and treats a greater variety of immunological control networks. Such topological models provide guidance for much more complicated continuous analyses using specific systems of differential equations.

## 2. Background

An immunological control network can be represented by a bipartite signed directed graph. The vertices of this graph represent distinguishable subsets of lymphocytes. The lymphocytes encountered in the models in this paper are helper and suppressor thymus-derived (T) lymphocytes (Th and Ts, respectively) and the so-called B lymphocytes. Each lymphocyte has an associated idio type which may be positive or negative corresponding to a coloring of the vertices of the graph in one of two colors. In the graphs used in this paper vertices associated with positive and negative idiotypes are represented by squares or rectangles and circles or ellipses, respectively.

The directed edges of the immunological control network represent interactions between lymphocytes in different subsets based on complementary idio type-antiidiotyp e interactions (Jerne, 1974). Thus edges can be directed only from a positive to a negative vertex or from a negative to a positive vertex. Edges between pairs of vertices of the same sign (i.e., positive to positive or negative to negative) are not possible. An immunological control network can

thus be represented by a bipartite graph. The directed edges are given positive or negative signs depending upon whether they represent help or suppression, respectively.

The vertices of an immunological control network can be classified as either strong or weak vertices. A strong vertex has at least one edge directed towards it and at least one edge directed away from it, e.g.



I

A weak vertex either has only edges directed towards it (a sink, IIa) or only edges directed away from it (a source, IIb),



IIa



IIb

Strong vertices represent internal variables and weak vertices represent external variables. A strong vertex with two or more edges directed towards it is called a turbulent vertex.

The relationships between the internal variables are of interest in the treatment of immunological control networks in this paper as well as in the previous work on chemical reaction networks (King, 1980, 1982, 1983). Such relationships are represented by signed directed graphs known as influence diagrams. An influence diagram is obtained from the corresponding immunological control network by deleting all of the weak vertices and any edges connected to weak vertices until only strong vertices remain. Such deleted weak vertices represent external

variables such as antigens (sources, e.g. 11b) or antibodies (sinks, e.g. 11a). Conversion of an immunological control network into the corresponding influence diagram can require several stages if removal of a weak vertex and its associated edges converts a strong vertex into a weak vertex.

This procedure is illustrated by the conversion of an immunological control network reported by DeLisi (1983) to the corresponding influence diagram (Figure 1). In the original network (Figure 1, top), the vertices A and B are weak vertices and SI, S, HI, H and  $M\phi$  are strong vertices. Removal of the vertices A and B and the associated four edges  $A \rightarrow SI$ ,  $A \rightarrow HI$ ,  $H \rightarrow B$ , and  $M\phi \rightarrow B$  leads to a network with the five vertices SI, S, HI, H and  $M\phi$ . (Figure 1, middle); all of these five vertices are strong vertices as required. In this case the relationship between the circuits in this diagram can be represented by a graph (e.g., Figure 1, bottom) in which both vertices are weak. This graph represents the relation between the suppressor T-cells (S+SI) and helper T-cells (H+HI) implied by the DeLisi model and shows the absence of feedback between these cells required to model immune responses. For this reason this model will not be treated in further detail in this paper.

The circuits in influence diagrams are important in the treatment of this paper. A circuit in an influence diagram consists of a path which starts with a given vertex and follows various edges in the directions of the arrows until the original vertex is reached again. The length of a circuit is the number of edges in the circuit that must be traversed from a given vertex until the same vertex is reached again. A circuit is negative if it has an odd number of negative edges and positive if it has an even number of negative edges or no negative edges. Following previous practice (King, 1980, 1982, 1983) positive and negative circuits of length n will be called  $B_n$  and  $C_n$  circuits, respectively. The bipartite graphs discussed in this paper can have circuits only of even lengths.

Now consider the dynamics of a system depicted by a given influence diagram as represented by the flow topology around an unstable equilibrium point. Possible flow topologies include one or more stable steady states as well as oscillations or chaos. The earlier work on chemical reaction networks focused on networks exhibiting periodic oscillations (King, 1980) or aperiodic chaos (King, 1983). The current work on immunological control networks, on the other hand, is concerned with networks proceeding from an initial virgin state by exposure to antigen to give one or more steady states corresponding, for example, to suppression or help configurations (Herzenberg, Black, Herzenberg, 1980). Suitable influence diagrams for modelling immunological control networks thus exhibit an appropriate number of stable configurations rather than oscillation or chaos.

The procedure for determining the flow topology corresponding to a given influence diagram uses methods based on switching circuit theory (Caldwell, 1958; Hu, 1968) as adapted by Glass and Kauffmann (1973), Glass (1975a, b, 1977a, b), and Glass and Pasternak (1978) and which have been termed kinetic logic (Thomas, 1979). In the logical description used in this approach time may be involved either synchronously (Glass and Kauffmann, 1973; Glass, 1975) or asynchronously (Thomas, 1984; Kaufman, Urbain, and Thomas, 1985). Since the special features of the more complicated asynchronous version (e.g., the effects of time delays) are not necessary for this work, the simpler synchronous version will be used throughout this paper. For simple influence diagrams such as those discussed in this paper both versions appear to give similar flow topologies.

Consider the immunological control network represented by an influence diagram as a synchronous switching network in which time is quantized so that the signs of the first time derivatives of the internal variables at time  $t+1$  are determined by their signs at time  $t$  (Glass, 1975a). The switching state at any time of such a network containing  $n$  internal variables can be represented by an  $n$ -dimensional vector of 1's and 0's corresponding to positive and negative

time derivatives, respectively, of the  $n$  internal variables. Such an  $n$ -vector is called a state vector. The number of different possible state vectors in an  $n$ -dimensional system is  $2^n$  and these state vectors can be represented by the  $2^n$  vertices of an  $n$ -dimensional cube. The possible transitions from states at synchronous time  $t$  to those at time  $t+1$  may then be represented by arrows directed along the edges of the  $n$ -dimensional cube. In such transitions the value of exactly one component of the state vector changes. Furthermore, in this synchronous treatment the discrete time scale  $t$  is chosen so that it advances one unit each time a single component of the state vector changes. The resulting  $n$ -dimensional cube with directed edges is called a state transition diagram. The center of the  $n$ -dimensional cube representing a state transition diagram corresponds to a steady state in which all of the first time derivatives of the internal variables are zero and therefore do not correspond to either Boolean variable 0 or 1. If this steady state is unstable, the transitions represented by the directed edges of the state transition diagram define the fundamental topology of the flow in the neighborhood of the unstable steady state.

The calculation of a state transition diagram corresponding to a given turbulent influence diagram can be performed by the following five-step procedure:

(1) A logical relation (OR or AND) is assigned between each pair of edges directed towards a given turbulent vertex. An OR relationship between arrows from vertices  $X$  and  $Y$  both going to a turbulent vertex  $Z$  implies that the internal variables  $X$  and  $Y$  affect the level of  $Z$  in separate processes corresponding to an equation of the general type

$$dZ/dt = aX^r + bY^s \quad (1)$$

An AND relationship between arrows from vertices  $X$  and  $Y$  both going to a

turbulent vertex Z implies that the internal variables X and Y affect the level of Z in the same process corresponding to an equation of the type

$$dZ/dt = aX^rY^s \quad (2)$$

The OR relationship at turbulent vertices corresponding to separate processes appears to be more realistic for influence diagrams based on immunological control networks (Kaufman, Urbain, and Thomas, 1985) and is used in this paper. In the case of influence diagrams modelling chemical reaction networks either OR or AND relationships at turbulent vertices may be realistic depending upon the nature of the chemical system.

(2) A local truth table is generated for each circuit in the influence diagram to indicate possible transitions between state vectors. In order to see how such a local truth table is generated, consider possible effects of one internal variable X on a second internal variable Y. If X helps Y as indicated by a positive arrow from X and Y in the circuit under consideration, then in the local truth table the values for Y in each possible state vector at time t+1 will correspond to the values for X at time t. If X suppresses Y as indicated by a negative arrow from X to Y in the circuit under consideration, then in the local truth table the values for Y in each possible state vector at time t+1 will be the opposite of the values for X at time t (i.e., a 0 for X at time t leads to a 1 for Y at time t+1 and vice versa).

(3) The local truth tables for each of the circuits in the influence diagram are combined to give a global truth table using the logical relationships at the turbulent vertices as follows:

(a) If any of the local truth tables show a value of 0 for a variable represented by an AND turbulent vertex, then the global truth table for that variable also

shows a value of 0.

(b) If any of the local truth tables show a value of 1 for a variable represented by an OR turbulent vertex, then the global truth table for that variable also shows a value of 1.

(4) Each state vector in the global truth table at time  $t+1$  is compared with the corresponding state vector at time  $t$ . If any such pair of state vectors are the same, then that state vector corresponds to a stable configuration of the immunological control network modelled by the influence diagram.

(5) If no stable configurations are found, then possibilities for oscillatory and/or chaotic behavior are explored by using the global truth table to determine the corresponding state transition diagram as discussed in a previous paper (King, 1983). Since this situation does not arise in the immunological control networks discussed in detail in this paper, the relevant algorithm will not be repeated here.

### 3. The Herzenberg Models

The Herzenberg models for immunological control networks (Herzenberg, Black and Herzenberg, 1980) use five independent variables: B cells, two types of helper T cells Th1 and Th2, and two types of suppressor T cells Ts1 and Ts2. Helper Th cells carry antiidiotypic  $V_H$  structures and thus correspond to negative vertices in the bipartite immunological control networks (ellipses in Figure 2). Suppressor Ts cells and B cells carry idiotypic  $V_H$  structures which are complementary to the antiidiotypic  $V_H$  structures and thus correspond to positive vertices in the bipartite immunological control networks (rectangles and squares in Figure 2). The soluble products of the Herzenberg models (e.g.,  $P_1$ ,  $P_2$ , and  $P_3$  in Eisenfeld and DeLisi, 1985) are viewed as dependent rather than independent

variables with their levels being so tightly coupled to B cells that they do not need to be considered as separate variables. In this way the number of variables in the Herzenberg models considered in this paper can be limited to five.

The Herzenberg models consist of a bistable core regulatory circuit (CRC) which can be maintained stably in either the help or suppression mode. One or more auxiliary regulatory circuits (ARC's) are linked to this CRC and can switch the CRC between the help and suppression modes.

The Herzenberg CRC is depicted in Figure 2 (top). It represents the simplest way of linking helper and suppressor T cells to satisfy the following conditions:

(1) Antiidiotypic cells can only interact with idiotypic cells or vice versa so that only bipartite graphs are allowed thereby excluding graphs containing circuits of odd lengths.

(2) The Th and Ts cells are differentiated so that the populations of target Th and helper Th for a given Ts are drawn from different Th populations.

The Herzenberg CRC (Figure 2, top) is thus seen to consist of a single positive circuit of length 4, called a fundamental quadrilateral (King, 1982). By a theorem in the previous paper (Theorem 8, in King, 1982), a positive fundamental quadrilateral must have two attracting regions or stable configurations exactly as suggested in the Herzenberg analysis.

In order to determine the nature of these two stable configurations the truth table for the Herzenberg CRC is determined (Table 1). The stable "help" configuration corresponds to a (Ts1, Th1, Ts2, Th2) state vector of (0, 1, 1, 0) or  $dTs1/dt < 0$ ,  $dTh1/dt > 0$ ,  $dTs2/dt > 0$ , and  $dTh2/dt < 0$ . In this configuration Th1 increases ( $dTh1/dt > 0$ ) and thus helps the differentiation of Ts2 (i.e.,  $dTs2/dt > 0$ ) which then depletes Th2 (i.e.,  $dTh2/dt < 0$ ), which in turn disables differentiation and expression of the Ts2 population (i.e.,  $dTs2/dt < 0$ ), which, if present and active, would be capable of attacking Th1. The stable "suppression"

configuration corresponds to a  $(Ts1, Th1, Ts2, Th2)$  state vector of  $(1, 0, 0, 1)$  or  $dTs1/dt > 0$ ,  $dTh1/dt < 0$ ,  $dTs2/dt < 0$ , and  $dTh2/dt > 0$  leading analogously to an increase in  $Th2$  and a decrease in  $Th1$ .

The shifting of the CRC between the help and suppression configurations can be accomplished by addition of an ARC. The simplest ARC's consist of a single strong vertex, corresponding to the B cells and their interactions with the Th cells through soluble products. The single strong ARC vertex can be linked to the CRC in two ways to preserve the bipartite nature of the entire network (Figure 2, middle and bottom). The first of these networks,  $B_4 + C_4$ , (Figure 2, middle) corresponds to the "suppressive ARC" Herzenberg model (Herzenberg, Black and Herzenberg, 1980: Scheme 2, p.5) and consists of two circuits of lengths 4 of opposite signs with two edges in common and a single turbulent vertex, namely  $Th2$ . This turbulent vertex is assigned the OR relationship since the interactions of B and  $Ts2$  with  $Th2$ , as indicated by the directed edges, are separate processes. The truth table for this  $B_4 + C_4$  network (Table 2) illustrates the process of first generating local truth tables for each circuit and then combining the local truth tables into a global truth table by using the logical relationships at turbulent vertices (King, 1983). From the global truth table in Table 2 only one of the 32 possible  $(Ts1, Th1, Ts2, Th2, B)$  state vectors, namely  $(1, 0, 0, 1, 0)$ , is seen to lead to a stable configuration. This stable configuration has  $dTs1/dt > 0$ ,  $dTh1/dt < 0$ ,  $dTs2/dt < 0$ , and  $dTh2/dt > 0$  corresponding to the stable "suppression" configuration of the isolated CRC (Table 1). This simple example, which corresponds to one of the Herzenberg networks, shows how addition of an ARC to a CRC can establish the CRC into one of its two stable configurations.

The other possible way of adding a single strong vertex (B) to the Herzenberg CRC while preserving the bipartite nature of the network (Figure 2, bottom) leads to a five-vertex  $B_4 + B_2$  network consisting of positive circuits of length

4 and 2 sharing a common vertex. This shared vertex (Th1) is thus turbulent and is assigned the OR relationship as in the  $B_4 + C_4$  case above. The truth table for this  $B_4 + B_2$  network (Table 3) indicates a single stable configuration corresponding to the stable "help" configuration of the isolated CRC (Table 1) with  $dTs1/dt < 0$ ,  $dTh1/dt > 0$ ,  $dTs2/dt > 0$ , and  $dTh2/dt < 0$  opposite to the stable "suppression" configuration of the  $B_4 + C_4$  network discussed above.

This analysis thus indicates simple ways of attaching a fifth vertex (B) to a given vertex (Th1) of the simple four-vertex Herzenberg CRC to lock it in either the "suppression" or "help" configurations. The help-stimulating Herzenberg network (Herzenberg, Black and Herzenberg, 1980: Scheme 3, p. 6) is a sum of the  $B_4 + C_4$  and  $B_4 + B_2$  networks in Figure 2 (middle and bottom) with the  $B_4 + B_2$  behavior obviously dominating (i.e., a greater weight of the  $B \rightarrow Th1$  edge relative to the  $B \rightarrow Th2$  edge). The allotype-suppressive Herzenberg network (Herzenberg, Black and Herzenberg, 1980: Scheme 4, p.8) is still more complicated consisting of a seven-vertex  $B_4 + C_4 + C_4 + B_2$  network having a triply turbulent Th1 vertex common to all four feedback circuits as well as a (doubly) turbulent Th2 vertex.

#### 4. The Model of Kaufman, Urbain, and Thomas

The model of Kaufman, Urbain and Thomas (1985) for an immunological control network uses five independent variables: B = B cells, H = Th = helper T cells, S = Ts = suppressor T cells, A = antibody, and E = antigen (epitope). The relationship between these five variables is depicted in the network at the top of Figure 3. In this network A and E are weak vertices and B, H, and S are strong vertices. Removal of the vertices A and E and the associated five edges  $E \rightarrow B$ ,  $E \rightarrow H$ ,  $E \rightarrow A$ ,  $B \rightarrow A$ , and  $H \rightarrow A$  leads to a network with the three vertices B,

H, and S. In this stage B becomes a weak vertex because of the removal of the only edge directed to B, namely  $E \rightarrow B$ . Thus a second stage involving the removal of the vertex B and associated edge  $B \rightarrow H$  is necessary to obtain a two-vertex influence diagram corresponding to the original five-vertex immunological control network.

At this point there arises the question of treating the loops at the vertices H and S representing self-interactions. Deletion of these loops leading to a simple  $C_2$  circuit (Figure 3, bottom left) is the simplest approach but results in the loss of important information. The flow topology of such a simple  $C_2$  circuit corresponds to limit cycle oscillation but such a system can also function as a biochemical switch (Glass and Kauffman, 1973). A more complicated but better approach is the replacement of these self-interaction loops with a positive circuit between two complementary idiotypes (Figure 3, bottom right). This influence diagram has the same four variables as the Herzenberg CRC (Figure 2, top). However, these variables are not only linked in different ways but also must be assigned different parities to preserve the bipartite nature of this graph. The feedback circuit structure of the influence diagram arising from the model of Kaufman, Urbain and Thomas (1985) is much more complicated than the simple  $B_4$  circuit of the Herzenberg CRC. As a result of this, all four vertices of the influence diagram (Table 3, bottom right) arising from the model of Kaufman, Urbain and Thomas (1985) are turbulent.

The truth table (Table 4) corresponding to this influence diagram (Figure 3, bottom right) can be determined by assigning OR relationships to each of the turbulent vertices. This leads to two stable configurations as was found for the analogous analysis of the Herzenberg CRC discussed above. One of the stable configurations corresponds to a  $(H_1, H_2, S_1, S_2)$  state vector of  $(0, 0, 1, 1)$  or  $dH_1/dt < 0$ ,  $dH_2/dt < 0$ ,  $dS_1/dt > 0$ , and  $dS_2/dt > 0$ . This corresponds to the "non-responsive" state of Kaufman, Urbain, and Thomas (1985) in which only

Ts cells are present. The other stable configuration corresponds to a (H1, H2, S1, S2) state vector of (1,1,1,1) or  $dH1/dt > 0$ ,  $dH2/dt > 0$ ,  $dS1/dt > 0$ , and  $dS2/dt > 0$ . This corresponds to the "memory" state of Kaufman, Urbain, and Thomas (1985) in which both Th and Ts cells are present. Thus this treatment of the Kaufman, Urbain and Thomas model agrees with the results of their treatment for the case of the absence of antigen (E). Since the weak antigen vertex (E) was deleted from the original network (Figure 3, top) in deriving the corresponding influence diagram (Figure 3, bottom right), this is the case to which the calculation in Table 4 corresponds. This also demonstrates the essential equivalence of the method in this paper to the method used by Kaufman, Urbain, and Thomas (1985) in a case where either method can be applied.

#### 5. Other Models

Two older models for immunological control networks have also been examined by the methods outlined in this paper. The model of Hiernaux (1977) consists of a cycle of  $C_2$  circuits of the antibodies  $Ab_k$  ( $1 \leq k \leq n$ ) with an "external"  $C_2$  circuit to the antigen (Ag) (Figure 4). Investigation of the simplest non-trivial bipartite case where  $n = 4$  and using OR relationships at the four turbulent vertices  $Ab_k$  ( $1 \leq k \leq 4$ ) indicates only one stable configuration corresponding to an (Ag, Ab1, Ab2, Ab3, Ab4) state vector of (0, 1, 1, 1, 1). The model of Richter (1978a, b) consists of an open chain of  $C_2$  circuits (Figure 5). Investigation of the flow topology of this system for  $n = 4$  reveals the absence of any stable configurations suggesting oscillatory behavior of this model. Hoffmann (1982) has already indicated difficulties of these models relating to the absence of the required stable configurations.

## 6. Summary

This paper shows that flow topological methods developed for the analysis of the dynamics of chemical reaction networks (King, 1980, 1982, 1983; Glass and Kauffmann, 1973; Glass, 1975a, b, 1977a, b; Glass and Pasternak, 1978) can also be used for the analysis of immunological control networks with appropriate modifications to account for the differences between the two types of networks. Thus the chemical reaction networks of interest have included systems exhibiting periodic oscillations or aperiodic chaos whereas the immunological control networks represent nonoscillatory systems having one or more stable configurations (e.g., "help" and/or "suppression"). In addition, the complementary idiotypic-antiidiotypic interactions in the immunological control networks lead to bipartite graphs, a feature not generally found in chemical reaction networks.

The Herzenberg models for immunological control networks (Herzenberg, Black, and Herzenberg, 1980) are most suitable for the methods outlined in this paper because of the presence of a minimum number of turbulent vertices. Flow topological analysis of the Herzenberg models leads to the locking in stable "help" and/or "suppression" configurations observed experimentally. In addition, the flow topology of the model of Kaufman, Urbain, and Thomas (1985) confirms the presence of the "memory" and "non-responsive" states found in their analysis indicating essential agreement of the two methods for the treatment of cases where both can be applied. However, the flow topologies of the models of Hiernaux (1977) and Richter (1978a, b) indicate the presence of only one and zero stable configurations, respectively, thereby suggesting major difficulties with these models in accord with their recent analysis of Hoffmann (1982). In any case this paper demonstrates the application of flow topology for the analysis of immunological control networks to reproduce some of the basic features of such

networks in simple systems using a few as four or five internal independent variables.

Acknowledgments: I am indebted to the Office of Naval Research for partial support of this work. I would also like to acknowledge helpful discussions with Prof. Jerome Eisenfeld (Department of Mathematics, University of Texas at Arlington) at the Conference on "Perspectives in Biological Dynamics and Theoretical Medicine" in Bethesda, Maryland, April, 1986.

REFERENCES

- CALDWELL, S.H. (1976). Switching Circuits and Logical Design (2nd Edition),  
New York: Wiley.
- CLARKE, B.L. (1980). Advan. Chem. Phys. **43**, 1-215.
- DE LISI, C. (1983). Ann. Rev. Biophys. Bioeng. **12**, 117-138.
- EISENFELD, J. (1986). N.Y. Acad. Sci. Proc. Conf. Perspectives in Biological  
Dynamics and Theoretical Medicine. in press.
- EISENFELD, J. and DE LISI, C. (1985). In: Mathematics and Computers in  
Biomedical Applications (Eisenfeld, J. and De Lisi, C. ed.), Amsterdam:  
Elsevier.
- GLASS, L. and KAUFFMAN, S.A. (1973). J. Theor. Biol. **39**, 103-129.
- GLASS, L. (1975a). J. Theor. Biol. **54**, 85-107.
- GLASS, L. (1975b). J. Chem. Phys. **63**, 1325-1335.
- GLASS, L. (1977a). In: Statistical Mechanics and Statistical Methods in Theory  
and Application (Landman, U. ed.), New York: Plenum.
- GLASS, L. (1977b). In: Statistical Mechanics, Pt. B (Berne, B.J. ed.), New York,  
Plenum.
- GLASS, L. and PASTERNAK, J.S. (1978). J. Math. Biol. **6**, 207-223.
- HERZENBERG, L.A., BLACK, S.J., and HERZENBERG, L.A. (1980). Eur. J.  
Immunol. **10**, 1-11.
- HIERNAUX, J. (1977). Immunochem. **14**, 733-739.
- HOFFMANN, G.W. (1978). In: Theoretical Immunology (Bell, G.I., Perelson,  
A.S., and Pimbley, G.H., eds.), New York: Marcel Dekker.
- HOFFMANN, G.W. (1982). in: Regulation of Immune Response Dynamics (DeLisi,  
C. and Hiernaux, eds.), Boca Raton, Florida: CRC Press.
- HU, S.-T. (1968). Mathematical Theory of Switching Circuits and Automata.

Berkeley and Los Angeles: California Press.

JERNE , N.K. (1974). Ann. Immunol. (Paris) **125C**, 373-389.

KAUFMAN, M., URBAIN, J., and THOMAS, R. (1985). J. Theor. Biol. **114**, 527-561.

KING, R.B. (1980). Theor. Chim. Acta (Berlin) **56**, 269-296.

KING, R.B. (1982). J. Theor. Biol. **98**, 347-368.

KING, R.B. (1983). Theor. Chim. Acta (Berlin), **63**, 323-338.

RICHTER, P.H. (1978a). In: Systems Theory in Immunology (Bruni, C., Doria, G., Koch, G. and Strom, R. eds.), New York: Springer-Verlag.

RICHTER, P.H. (1978b). In: Theoretical Immunology (Bell, G.I., Perelson, A.S., and Pimpley, G.H. eds.), New York: Marcel Dekker.

THOMAS, R. (1979). Kinetic Logic. Berlin:Springer.

THOMAS, R. (1984). Adv. Chem. Phys. **55**, 247.

TABLE 1  
TRUTH TABLE FOR THE HERZENBERG CRC

Time t				Time t+1				
Ts1	Th1	Ts2	Th2	Ts1	Th1	Ts2	Th2	
0	0	0	0	0	1	0	1	
0	0	0	1	1	1	0	1	
0	0	1	0	0	1	0	0	
0	0	1	1	1	1	0	0	
0	1	0	0	0	1	1	1	
0	1	0	1	1	1	1	1	
0	1	1	0	0	1	1	0	stable configuration ("help")
0	1	1	1	1	1	1	0	
1	0	0	0	0	0	0	1	
1	0	0	1	1	0	0	1	stable configuration ("suppression")
1	0	1	0	0	0	0	0	
1	0	1	1	1	0	0	0	
1	1	0	0	0	0	1	1	
1	1	0	1	1	0	1	1	
1	1	1	0	0	0	1	0	
1	1	1	1	1	0	1	0	





TABLE 4

TRUTH TABLE FOR THE MODEL OF KAUFMAN, URBAIN, AND THOMAS

<u>Time, t</u>			<u>Local (Right C<sub>4</sub>)</u>			<u>Local (Left C<sub>4</sub>)</u>			<u>Global (All OR)</u>		
<u>H1</u>	<u>H2</u>	<u>S1 S2</u>	<u>H1</u>	<u>H2</u>	<u>S1 S2</u>	<u>H1</u>	<u>H2</u>	<u>S1 S2</u>	<u>H1</u>	<u>H2</u>	<u>S1 S2</u>
0	0	0 0	1	0	0 0	0	1	0 0	1	1	0 0
0	0	0 1	0	0	0 0	0	1	1 0	0	1	1 0
0	0	1 0	1	0	0 1	0	0	0 0	1	0	0 1
0	0	1 1	0	0	0 1	0	0	1 0	0	0	1 1
0	1	0 0	1	0	1 0	1	1	0 0	1	1	1 0
0	1	0 1	0	0	1 0	1	1	1 0	1	1	1 0
0	1	1 0	1	0	1 1	1	0	0 0	1	0	1 1
0	1	1 1	0	0	1 1	1	0	1 0	1	0	1 1
1	0	0 0	1	1	0 0	0	1	0 1	1	1	0 1
1	0	0 1	0	1	0 0	0	1	1 1	0	1	1 1
1	0	1 0	1	1	0 1	0	0	0 1	1	1	0 1
1	0	1 1	0	1	0 1	0	0	1 1	0	1	1 1
1	1	0 0	1	1	1 0	1	1	0 1	1	1	1 1
1	1	0 1	0	1	1 0	1	1	1 1	1	1	1 1
1	1	1 0	1	1	1 1	1	0	0 1	1	1	1 1
1	1	1 1	0	1	1 1	1	0	1 1	1	1	1 1

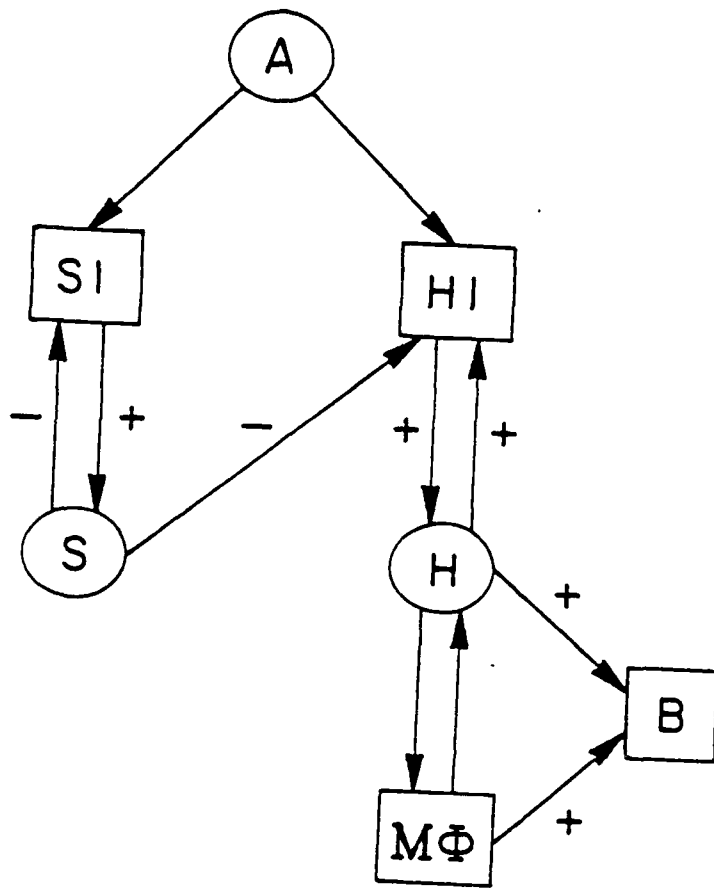
stable configuration "non-responsive"

stable configuration "memory"

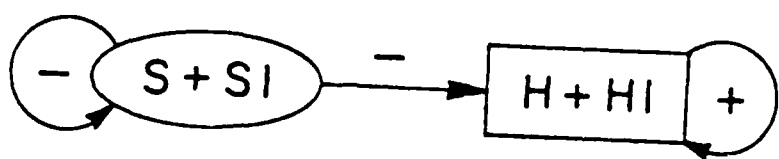
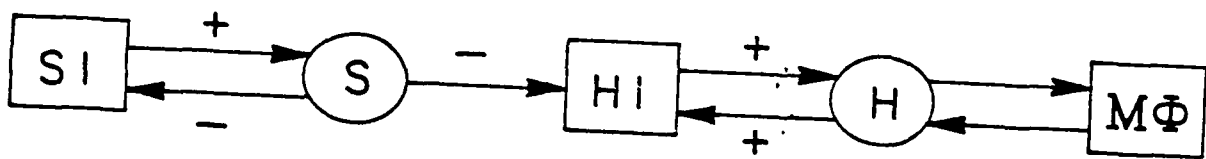
Figure 1: The immunological control network of DeLisi (1983). (a) Top: the original seven-vertex directed graph; (b) Middle: removal of the weak vertices A and B and the associated edges  $A \rightarrow SI$ ,  $A \rightarrow HI$ ,  $H \rightarrow B$ , and  $M\phi \rightarrow B$ ; (c) Bottom: the corresponding two-vertex signed directed graph in which the (weak) vertices  $S + SI$  and  $H + HI$  correspond to suppressor and helper T cells, respectively.

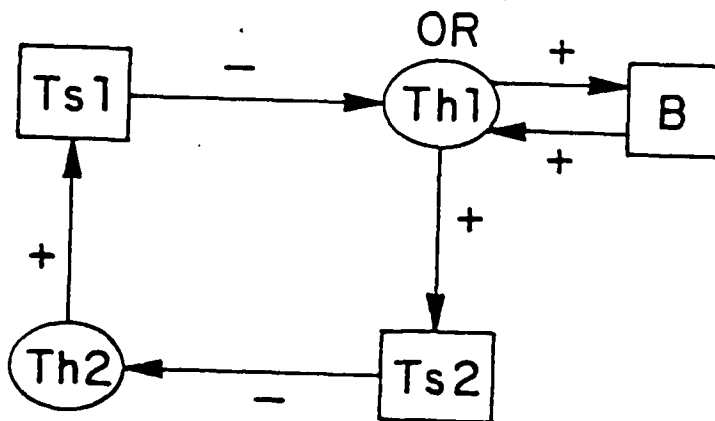
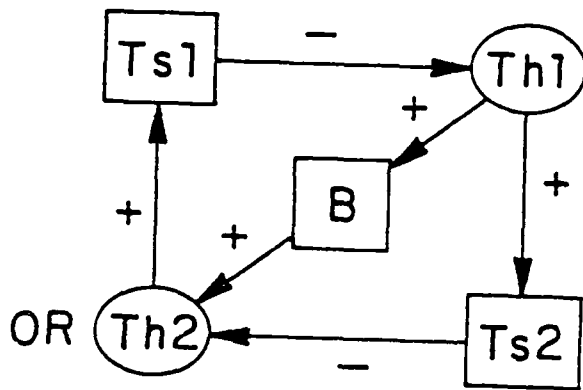
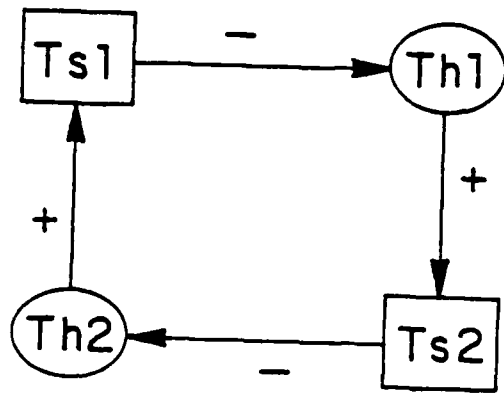
Figure 2: Influence diagrams corresponding to the Herzenberg models (Herzenberg, Black and Herzenberg, 1980). (a) Top: the four-vertex CRC; (b) Middle: addition of a fifth vertex (B) to give the  $B_4 + C_4$  system stabilizing the "suppression" configuration; (c) Bottom: addition of a fifth vertex (B) to give the  $B_4 + B_2$  system stabilizing the "help" configuration.

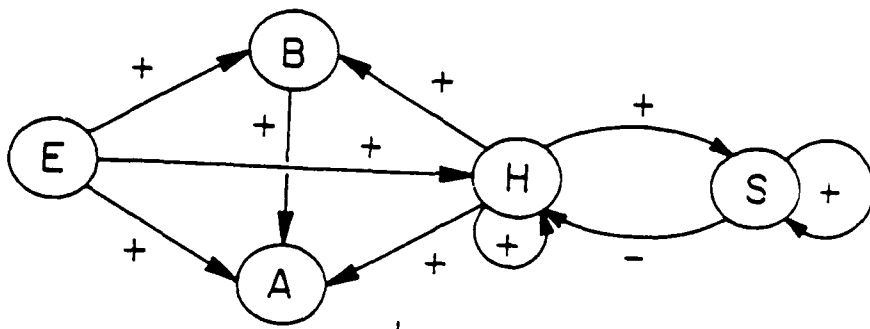
Figure 3: The immunological control network of Kaufman, Urbain, and Thomas (1985). (a) Top: the original five-vertex signed directed graph; (b) Upper middle: removal of the weak vertices E and A as well as the loops at H and S to give a three-vertex signed directed graph; (c) Lower middle: removal of the weak vertex B and the edge  $B \rightarrow H$  from the three-vertex signed directed graph to give a two-vertex signed directed graph; (d) Bottom left: removal of the positive loops at H and S; (e) Bottom right: replacement of the positive loops at H and S with positive circuits between the two complementary idotype pairs  $H1/H2$  and  $S1/S2$  respectively.



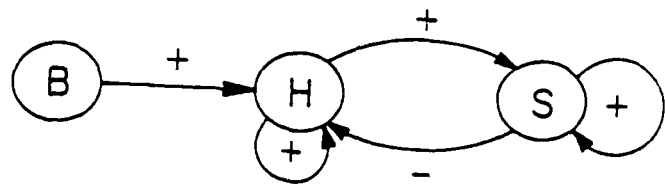
-A, B







-EA



-B

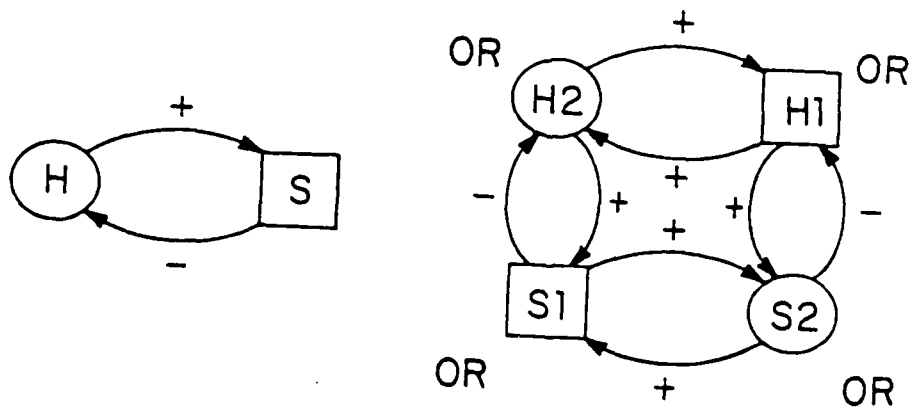
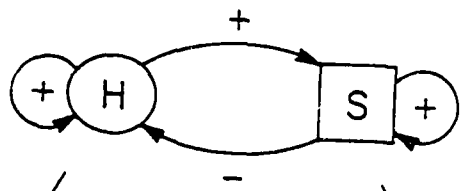
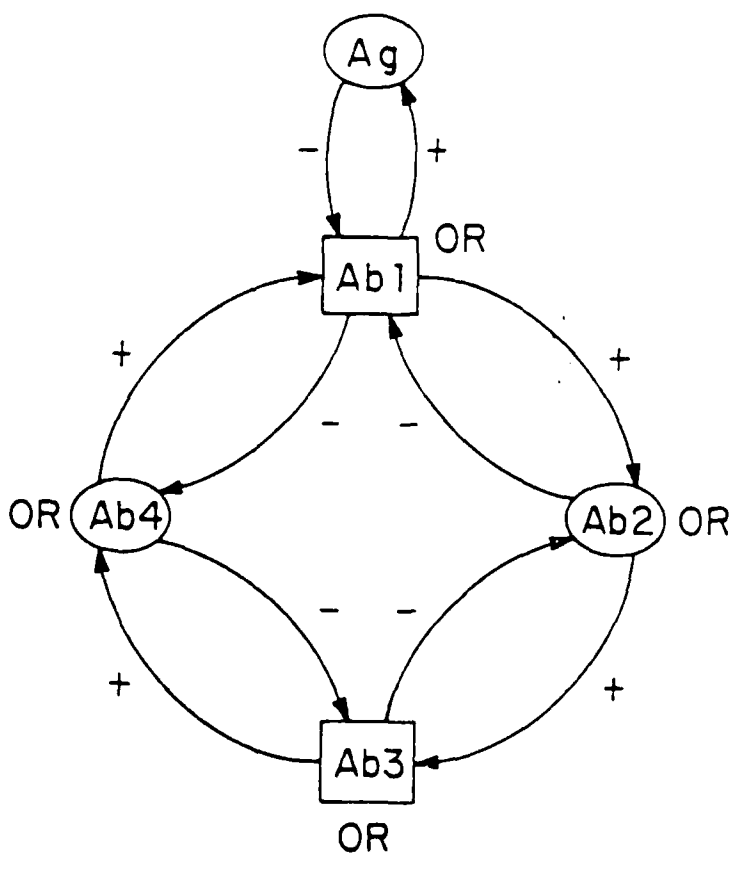
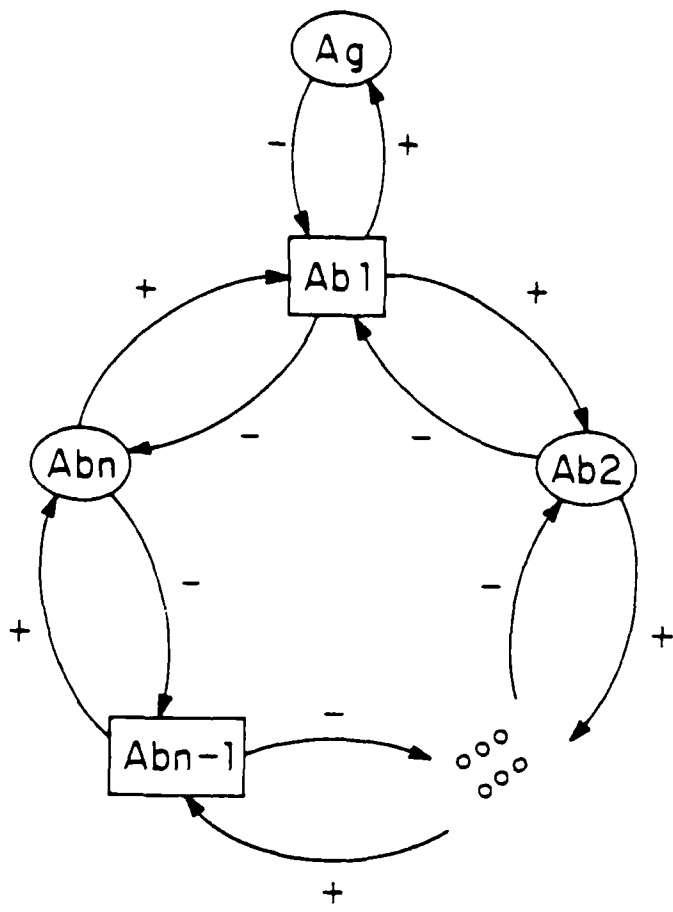
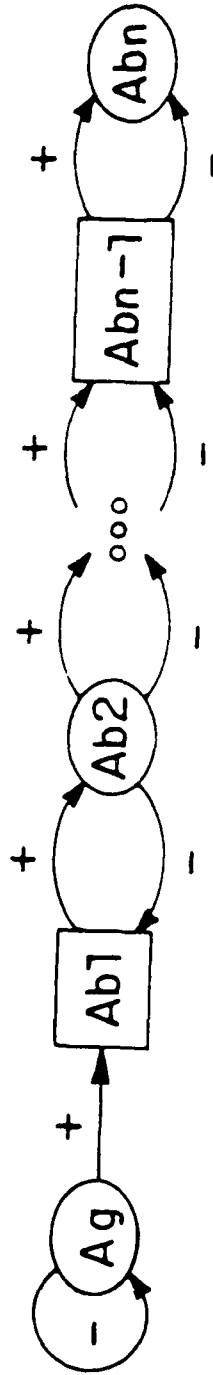


Figure 4: The immunological control network of Hiernaux (1977): (a) Top: the general case; (b) Bottom: the simplest non-trivial bipartite case of this network where  $n = 4$  with OR relationships at the four turbulent vertices  $A_{bk}$  ( $1 \leq k \leq 4$ ).

Figure 5: The immunological control network of Richter (1978).





TECHNICAL REPORT DISTRIBUTION LIST, GEN

	<u>No. Copies</u>		<u>No. Copies</u>
Office of Naval Research Attn: Code 1113 800 N. Quincy Street Arlington, Virginia 22217-5000	2	Dr. David Young Code 334 NORDA NSTL, Mississippi 39529	1
Dr. Bernard Douda Naval Weapons Support Center Code 50C Crane, Indiana 47522-5050	1	Naval Weapons Center Attn: Dr. Ron Atkins Chemistry Division China Lake, California 93555	1
Naval Civil Engineering Laboratory Attn: Dr. R. W. Drisko, Code L52 Port Hueneme, California 93401	1	Scientific Advisor Commandant of the Marine Corps Code RD-1 Washington, D.C. 20380	1
Defense Technical Information Center Building 5, Cameron Station Alexandria, Virginia 22314	12 high quality	U.S. Army Research Office Attn: CRD-AA-IP P.O. Box 12211 Research Triangle Park, NC 27709	1
DTNSRDC Attn: Dr. H. Singerman Applied Chemistry Division Annapolis, Maryland 21401	1	Mr. John Boyle Materials Branch Naval Ship Engineering Center Philadelphia, Pennsylvania 19112	1
Dr. William Tolles Superintendent Chemistry Division, Code 6100 Naval Research Laboratory Washington, D.C. 20375-5000	1	Naval Ocean Systems Center Attn: Dr. S. Yamamoto Marine Sciences Division San Diego, California 92132	1

END  
DATE  
FILMED  
MARCH  
1988  
DTIC